On the exploitation of multimodal remote sensing data combination for mesoscale/submesoscale eddy detection in the marginal ice zone

Eduard Khachatrian, Nikita Sandalyuk

Abstract—The detection and analysis of ocean eddies via remote sensing have become a hot topic in physical oceanography during the last few decades. However, eddy identification and tracking via remote sensing can be a challenging task since each sensor has some limitations. In order to overcome potential challenges, it is crucial to exploit the complementary information provided by different sensing systems. As one of the steps towards this aim, we have investigated the pertinence of applying the scheme including texture features extraction and superpixel segmentation method in order to distinguish eddies in the marginal ice zone using multisensor remote sensing data. Nevertheless not all the images available from various sensors are of actual importance since they can be corrupted, redundant, or simply unnecessary for a particular task. Therefore, we are additionally exploring the relevance of different sensors separately and simultaneously as well as with extracted texture features for eddy monitoring.

Index Terms—Eddy monitoring; remote sensing; synthetic aperture radar, marginal ice zone; superpixel segmentation; GLCM texture features

I. INTRODUCTION

Eddies appear everywhere in the ocean. They have horizontal dimensions from several to hundreds of kilometers and vertical scales of hundreds of meters [1]. The eddies trap water and transport momentum, volume, heat, salt, and biogeochemical constituents. A single eddy may transport a trillions of tons of water and tens of terajoules of heat from their generation regions to dissipation sites [1], [2], [3].

Over the past 30 years and to this day, satellite radar altimetry has been the main source of the information about the ocean eddies. The merged datasets from different altimetry missions used to construct the gridded sea level anomaly (SLA) fields are a great tool to study mesoscale eddies. The advent of various automated eddy detection algorithms and their implementation to the SLA fields allowed scientist to acquire an unprecedented amount of statistical data on the physical and kinematic properties of eddies [1], [4], [5]. However, the minimal size of the detected eddies is still limited by the spatial resolution of the gridded SLA fields [1]. On the other hand, the undetectable by satellite altimetry mesoscale and submesoscale eddies greatly contribute to the heat and salt fluxes in the regions of high eddy activity and these processes are still significantly understudied [6].

Eduard Khachatrian is with the Department of Physics and Technology, UiT The Arctic University of Norway, NO-9037 Tromsø, Norway, e-mail: eduard.khachatrian@uit.no. Nikita Sandalyuk is with Saint Petersburg State University, Saint Petersburg, Russia, e-mail: nikitasandaliuk@gmail.com.

This is particularly important for the seas in the polar areas due to its remote location, spatially and temporally sparse in situ observations,presence of sea ice, and significantly smaller Rossby radius of deformation compared to the mid-latitude oceans [7], [8].

Besides the satellite radar altimeters, there are other remote sensing sensors that can be used to observe different ocean surface phenomena. Optical sensors provide information about the region of interest in visible, infrared, and short-wave infrared intervals of the electromagnetic spectrum. The main advantage of such sensors is easy visual interpretability, however, optical sensors are limited to cloud-free and favorable light conditions, which can cause a significant problem, especially for polar areas, where dense cloud covers and long periods of darkness prevail for several months of the year [9]. On the other hand, spaceborne synthetic aperture radar (SAR) is independent of cloud and light conditions, which makes it the main sensor that can be applied for operational applications in polar areas [10]. There were some attempts to automatize the eddy detection using SAR [11], however, the automatic interpretation of remote sensing data, especially SAR data, is still challenging and strongly relies on experts' knowledge. Nevertheless, both optical and SAR sensors provide imagery with a high spatial resolution that allows detecting mesoscale and submesoscale eddies and favorably differentiate them from the data obtained using satellite altimetry. Notwithstanding, altimeters provide the datasets with significantly coarser spatial resolution than the aforementioned sensors, their main advantage is spatial coverage, therefore, they are more commonly used for global or large-scale observations.

Mesoscale and submesoscale eddies in the region of the Greenland Sea play crucial role in the heat and salt transport [8]. Moreover, eddies can have a significant impact on the sea ice concentration in the marginal ice zone (MIZ) in the Arctic Seas. In the area of Greenland Shelf the eddies sweep sea ice and advect warm Atlantic Water (AW) closer to the ice edge resulting in increased sea ice melt [12], [13]. In spite of the climatic importance, this region is still largely understudied in terms of submesoscale-mesoscale dynamics. The MIZ is defined as the transitional zone between the open water and dense drift ice. Various observations on MIZ become significantly important due to the fact that this area plays a crucial role in sea cover fluctuations, ice-ocean-atmosphere interactions, and climate in general [14]. Moreover, MIZ is the region with high intensity of dynamic processes with ice drift, ice eddies, wave-ice interaction, and intense biological
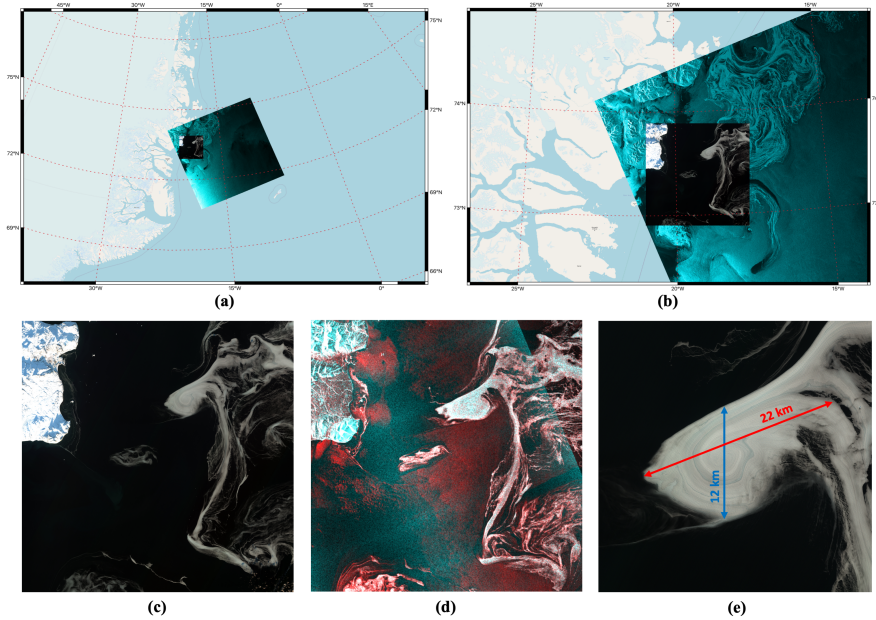
Figure 1: Study area around the Greenland Sea, East Greenland and locations of the images acquired from Sentinel-1 and Sentinel-2 satellites (**a, b**). Color representation of multisensor dataset: optical natural-color composite (RGB) (**c**) and SAR false-color composite (HH, HV and HV as RGB) (**d**), as well as size of the eddy used in this study (**e**). Both scenes were acquired on 18 October 2021.

activity, that are active areas of shipping and fishery.

In the work [6] authors presented a comprehensive quantitative analysis of eddy characteristics in the seasonally ice-free and MIZ regions for the Western Artic Ocean. The possibility of the retrieval of horizontal eddy velocities in the MIZ region was demonstrated in the study [15]. It should be noted, that there were attempts to apply various automatic machine learning techniques for eddy identification applying commonly used altimetry data [16], [17] and some attempts employing SAR data [18]. Nevertheless, so far, the eddy detection in the Arctic region was mostly based on the visual inspection of the satellite images [6], [8]. However, it is clear that the human supervised method of eddy detection based only on the SAR images could contain various biases [6]. The same applies to automatic monitoring of eddies using remote sensing data, especially using SAR data, which is challenging and strongly relies on experts' knowledge. Therefore, there is a clear necessity to apply multisensor datasets that can be useful both for manual and automatic eddy monitoring. Multisensor remote sensing refers to the use of various sensors usually operating at different frequencies and/or spatial resolutions and coverage. Diverse remote sensing sensors can grasp various properties of the region of interest (ROI) by using different physical principles. Furthermore, combining the information from multiple sensors allows better characterization and provides unique information regarding the region of interest [19].

In this study, we explore the potential of applying multisensor datasets for mesoscale-submesoscale eddy monitoring, as well as examining the complementary information provided by each sensor separately and simultaneously. To achieve this objective we choose one randomly selected individual eddy which is perfectly detectable from all sensors as a test case study and implemented various image processing

techniques, namely texture feature extraction and superpixel segmentation. Moreover, we study the potential of operational eddy monitoring using only publicly available remote sensing datasets. It should be additionally noted that the main purpose of our study is not to obtain as much information as possible about quantitative eddy characteristics in the study region but rather to collect important information on the possibility of the multisensor data for retrieving eddy properties.

The rest of this paper is organized as follows. Section II describes the dataset and method used in this study. Section III presents an analysis and experimental results. Finally, the discussion and conclusions are presented in Section IV.

II. DATASET AND METHOD DESCRIPTION

The following section describes the dataset, consisting of SAR and optical images that were used in this study as well as methods performed for its processing.

A. Dataset

The dataset includes SAR data obtained from Sentinel-1 and optical data obtained from Sentinel-2 acquired over the Greenland Sea on 18 October 2021. It should be noted, that both scenes are publicly available through Copernicus Open Access Hub (European Union's Earth observation programme). SAR dataset was generated from Sentinel-1 imagery in extra-wide (EW) swath mode at dual-polarization (HH and HV). It is worth mentioning, that Sentinel-1 operates at C-band (central frequency of 5.404 GHz) and includes two polar-orbit Sentinel-1A and Sentinel-1B missions that are able to work at multiple sensing modes. The optical dataset obtained from Sentinel-2 consists of 13 bands in the visible, near-infrared, and shortwave infrared parts of the spectrum. Sentinel-1 data have a pixel size of 40 m, while the pixel size of Sentinel-2
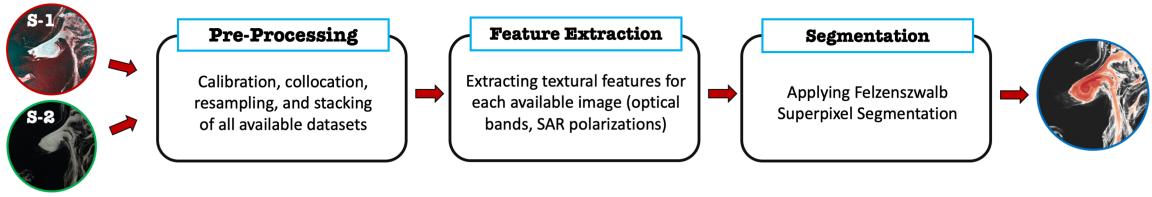
Figure 2: Flowchart describing the crucial steps that we used in this study. S-1 refers to the SAR data obtained from Sentinel-1, while S-2 corresponds to the optical data acquired from Sentinel-2.

varies from 10 m to 60 m depending on the spectral band. Both Sentinel-1 and Sentinel-2 datasets were collocated and resampled to the same pixel size of 60 m. Moreover, the Sentinel-1 data was denoised and calibrated to sigma-nought.

Figure 1 (a, b) illustrates the study area over the Greenland Sea, East Greenland. It should be noted that only the overlapping area of two datasets was used. Accordingly, the Figure 1 additionally shows the color representation of multisensor dataset: natural-color composite of Sentinel-2 (c) and false-color composite of Sentinel-1 (d), as well as the size of the eddy (e).

B. Method

Figure 2 shows the flowchart of the scheme that we used in this paper with several main steps that are described in the following subsections.
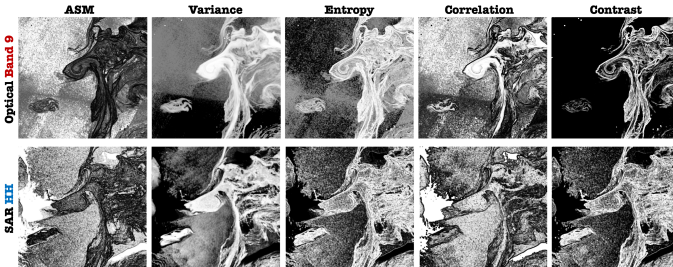
Figure 3: Examples of several GLCM texture features (ASM, variance, entropy, correlation, contrast) used in the proposed scheme extracted from optical Band 9 and SAR HH polarization.

1) Pre-Processing: The images acquired by various sensors might have different characteristics, such as units of measurement, spatial resolution, geographical coordinate systems, and etc. Thus the crucial first step is to make the data compatible by means of calibrating, collocating, and resampling to the same resolution. Moreover, in order to increase the accuracy of analysis and partly remove the noise, especially from the first sub-swath, we perform thermal noise removal as a pre-processing step for Sentinel-1 data using the ESA's Sentinel Application Platform (SNAP).

2) Feature Extraction: In order to increase the knowledge regarding the region of interest as well as extract some additional unique information from the original data, along with the bands of optical and SAR polarizations, we extracted texture features. Accordingly, for each image layer of SAR and optical (band and/or polarization) we extract the texture features using the Gray-Level Co-Occurrence Matrix (GLCM)

[20], [21]. We use the directional average for 0°, 45°, 90°, and 135° which is common practice to account for the possible rotation of structures or roughness patterns on the ocean surface. Therefore, for each available image, except optical band 10 (shortwave infrared cirrus), which was corrupted and thus, redundant for the analysis, i.e. 12 optical spectral bands and 2 SAR polarizations, we extracted 10 texture features, namely contrast, homogeneity, dissimilarity, angular second momentum (ASM), energy, entropy, maximum probability, mean, variance, and correlation. The final dataset consists of 154 collocated and cropped images merged together. Figure 3 illustrates several examples of extracted features that were used in this study. It is evident that texture features are providing supplementary unique information that can potentially improve existing methods of eddy detection in the SAR images and can be used for different applications. Moreover, each of the features separately can be applied to describe different characteristics of the eddy, for instance, contrast is giving a more clear overview regarding the eddy boundaries and vorticity.

3) Segmentation: Superpixel segmentation is grouping the pixels that share similar information together, which allows us to obtain homogeneous areas. This step can be achieved using different algorithms, such as Watershed [22], [23] or simple linear iterative clustering (SLIC) [24]. However, in our study, we are implementing Felzenszwalb [25] since it produces more accurate segments/superpixels for eddy identification. Superpixel segmentation allows separating the eddies in the marginal ice zone from other sea ice formations and open water. Eventually, the segmented map provides unique information regarding the eddies that can be further used for different applications.

III. ANALYSIS & EXPERIMENTAL RESULTS

The following section demonstrates the performance comparison between different data combinations as well as other experimental analyses and results.

A. Sensors Performance Comparison

In this section, we are comparing the performance of various sensors when used separately and simultaneously. Accordingly, we performed Felzenszwalb superpixel segmentation algorithm to different data combinations. Figure 4 illustrates segmented maps for three cases: (a) only Sentinel-2 bands, (b) only Sentinel-1 polarizations, and (c) combined SAR and optical data with extracted texture features for each attribute.
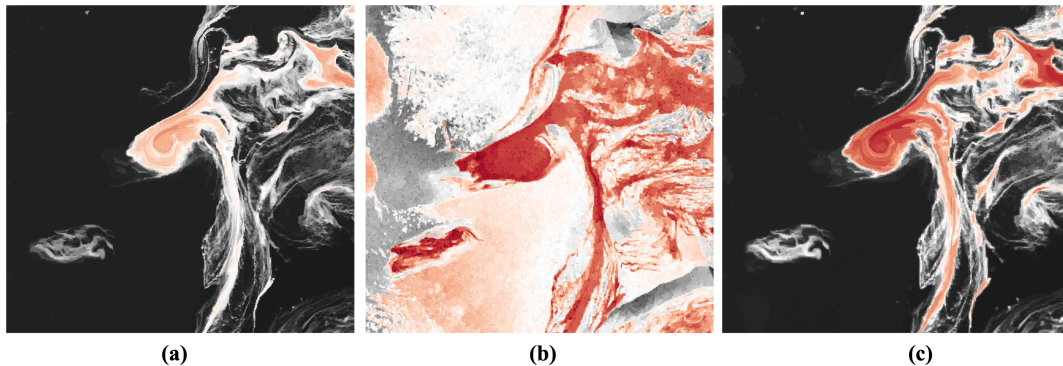
Figure 4: Segmented maps using Felzenszwalb superpixel segmentation algorithm for different data combinations: only optical bands (**a**), only SAR polarizations (**b**), and combined dataset + extracted GLCM texture features for each attribute (**c**), Greenland Sea, East Greenland, 18 October 2021.

It is worth mentioning that the cyclonic eddy identified in this study, can be also detected on the altimetry maps. However, we do not consider here a comparison of obtained eddy characteristics with altimetry data since gridded altimetry products have certain limitations and mapping errors due to the spatiotemporal gaps in altimetry tracks. Thus, we employed a test case that contains multisensor data that is publicly available in high resolution, especially in comparison to altimetry.

For the segmented map obtained with optical attributes, the eddy area is approximately equal to 173,8 km^2 with a longitudinal and latitudinal diameter of 13 and 16 km, respectively. A segmented map obtained using only SAR attributes provides similar information about the size of the eddy, namely an area equal to 178,2 km^2 , with a longitudinal and latitudinal diameter of 12 and 22 km, respectively.

It is visible from the segmented maps, that for each case the cyclonic eddy is well identified and clearly distinguished from the open water areas. For the optical case, the structure of the eddy, as well as its boundaries, are clearly separable. Whereas in the SAR case, the eddy is still separated from the calm water areas, however, there is significantly less information regarding the vorticity in the middle of the eddy, than in the segmented map obtained by the optical dataset. Moreover, for the SAR case, the result is highly affected by speckle and thermal noise which is one of the main limitations of this sensor in general. The combined case produces a bit different result, however, it has all the unique advantages of the segmented map obtained by the optical dataset. It is worth mentioning that for both optical and combined cases, the open water areas result in a more homogeneous area that allows to better separate other sea ice and water formations. It is evident that each of the sources can provide different complementary information, however, it should be noted, that there are still some limitations, especially for the operational eddy monitoring or identification. Even though optical data produces such a comprehensive result and outperforms the SAR data, it cant be used for operational eddy monitoring because it is highly dependent on the weather conditions in the ROI. SAR imagery on the contrary can be potentially used in any weather or light conditions, however, it is more complicated to interpret and highly affected by noise. Eventually, it is crucial to integrate both sensors in the eddy monitoring algorithms.
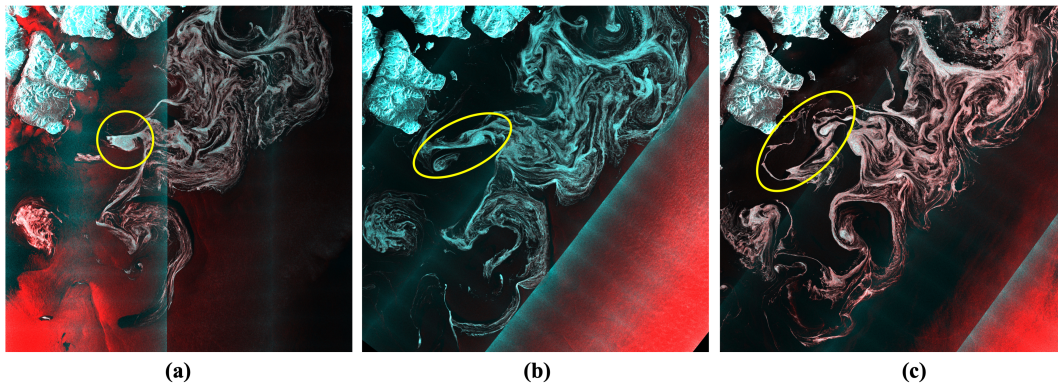
B. Eddy Evolution

Figure 5 demonstrates several sequential SAR images that illustrate the evolution of the cyclonic eddy that was analyzed in our study. We can see from the false-color composites that the detected eddy was formed along the stream of the East Greenland Current (EGC). The identified eddy is quickly dissipating and splitting into the separate smaller structures which is consistent with the previous studies that showed that the MIZ along the EGC is found to be both, a region of a relatively low eddy kinetic energy (EKE) and less energetic eddies [8]. The images also reveal the surface signatures of large number of elongated filaments and meanders which is typical manifestation of the mesoscale and submesoscale activity in the MIZ. Apparently, there are several eddies that can be also detected in the area bounded by 73-74°N and 18-15°E. It should be noted, that for 19-20 of October there were no suitable Sentinel-2 images due to dense cloud coverage. That once more illustrates the importance of the SAR sensor as a main source for monitoring evolution, dynamics, and fluctuations of eddies in the MIZ.

IV. CONCLUSIONS

In this paper, we explored the possibility of eddy monitoring in the MIZ using different multisensor data combinations that are publicly available. Additionally, we tried to compare the information relevance provided by each sensor separately and simultaneously. Moreover, we tried to introduce several techniques that are not commonly used for eddy monitoring, namely GLCM texture extraction and superpixel segmentation by creating a scheme that can be employed for different applications.

Furthermore, our results show how the information provided from various sensors differs and the importance of applying multisensor datasets for the purposes of eddy mesoscale-submesoscale monitoring. Additionally, we clearly demonstrated the advantages of applying the GLCM texture features for the eddy monitoring as well as employing superpixel segmentation that can be used as a tool both in automatic methods and for eddy experts working manually. We did not

Figure 5: Three sequential SAR false-color composites that are illustrating the evolution of the eddy in the marginal ice zone: (**a**) 18 October, (**b**) 19 October, (**c**) 20 October. The yellow ellipses indicate the exact location of the eddy that we analyzed in this paper.

yet investigate how our results are affected by the observation conditions, however, we are planning to do it in future works. Here we focused on the test case in order to explore the potential of multisensor data fusion for eddy monitoring and operational capabilities. From the experiments, it is clear that optical imagery provides a better result, however, the operational capabilities of optical sensors are very limited and can only be used under favorable light and cloud conditions. Therefore, we are showing that using both sensors, depending on their availability, will result in more accurate eddy monitoring since both sensors are able to provide complementary information.

REFERENCES

[1] D. B. Chelton, M. G. Schlax, and R. M. Samelson, "Global observations of nonlinear mesoscale eddies," *Progress in Oceanography*, vol. 91, no. 2, pp. 167–216, 2011.

[2] C. Wunsch, "Where do ocean eddy heat fluxes matter?," *Journal of Geophysical Research: Oceans*, vol. 104, no. C6, pp. 13235–13249, 1999.

[3] S. R. Jayne and J. Marotzke, "The oceanic eddy heat transport," *Journal of Physical Oceanography*, vol. 32, no. 12, pp. 3328 – 3345, 2002.

[4] A. Doglioli, B. Blanke, S. Sabrina, and G. Lapeyre, "Tracking coherent structures in a regional ocean model with wavelet analysis: Application to cape basin eddies - art. no. c05043," *Journal of Geophysical Research: Oceans*, vol. 112, 05 2007.

[5] J. Faghmous, I. Frenger, Y. Yao, R. Warmka, A. Lindell, and V. Kumar, "A daily global mesoscale ocean eddy dataset from satellite altimetry," *Scientific Data*, vol. 2, p. 150028, 06 2015.

[6] I. E. Kozlov, A. V. Artamonova, G. E. Manucharyan, and A. A. Kubryakov, "Eddies in the western arctic ocean from spaceborne sar observations over open ocean and marginal ice zones," *Journal of Geophysical Research: Oceans*, vol. 124, no. 9, pp. 6601–6616, 2019.

[7] G. Nurser and S. Bacon, "Eddy length scales and the rossby radius in the arctic ocean," *Ocean Science Discussions*, vol. 10, pp. 1807–1831, 10 2013.

[8] I. Bashmachnikov, I. Kozlov, L. Petrenko, N. Glock, and C. Wekerle, "Eddies in the north greenland sea and fram strait from satellite altimetry, sar and high-resolution model data," *Journal of Geophysical Research: Oceans*, 07 2020.

[9] S. Sandven, O. M. Johannessen, and K. Kloster, "Sea Ice Monitoring by Remote Sensing," *Encyclopedia of Analytical Chemistry*, vol. 1993, no. March 1993, pp. 1–43, 2006.

[10] A. Moreira, P. Prats-Iraola, M. Younis, G. Krieger, I. Hajnsek, and K. P. Papathanassiou, "A tutorial on synthetic aperture radar," *IEEE Geoscience and Remote Sensing Magazine*, vol. 1, no. 1, pp. 6–43, 2013.

[11] S. Karimova, "An approach to automated spiral eddy detection in sar images," in *2017 IEEE International Geoscience and Remote Sensing Symposium (IGARSS)*, pp. 743–746, 2017.

[12] V. Selyuzhenok, I. Bashmachnikov, R. Ricker, A. Vesman, and L. Bobylev, "Sea ice volume variability and water temperature in the greenland sea," *The Cryosphere*, vol. 14, no. 2, pp. 477–495, 2020.

[13] G. E. Manucharyan and A. F. Thompson, "Submesoscale sea ice-ocean interactions in marginal ice zones," *Journal of Geophysical Research: Oceans*, vol. 122, no. 12, pp. 9455–9475, 2017.

[14] D. Lubin and R. Massom, *Polar Remote Sensing: Volume I: Atmosphere and Oceans*. 01 2006.

[15] I. E. Kozlov, E. V. Plotnikov, and G. E. Manucharyan, "Brief communication: Mesoscale and submesoscale dynamics in the marginal ice zone from sequential synthetic aperture radar observations," *The Cryosphere*, vol. 14, no. 9, pp. 2941–2947, 2020.

[16] X. Chen, G. Chen, L. Ge, B. Huang, and C. Cao, "Global Oceanic Eddy Identification: A Deep Learning Method From Argo Profiles and Altimetry Data," *Frontiers in Marine Science*, vol. 8, no. May, pp. 1–15, 2021.

[17] K. Franz, R. Roscher, A. Milioto, S. Wenzel, and J. Kusche, "Ocean eddy identification and tracking using neural networks," in *IGARSS 2018 - 2018 IEEE International Geoscience and Remote Sensing Symposium*, pp. 6887–6890, 2018.

[18] D. Zhang, M. Gade, and J. Zhang, "Sar eddy detection using mask-rcnn and edge enhancement," in *IGARSS 2020 - 2020 IEEE International Geoscience and Remote Sensing Symposium*, pp. 1604–1607, 2020.

[19] M. Dalla Mura, S. Prasad, F. Pacifici, P. Gamba, J. Chanussot, and J. A. Benediktsson, "Challenges and opportunities of multimodality and data fusion in remote sensing," *Proceedings of the IEEE*, vol. 103, pp. 1585–1601, Sep. 2015.

[20] R. Haralick, K. Shanmugam, and I. Dinstein, "Texture features for image classification," *IEEE Transactions on Systems, Man, and Cybernetics*, vol. 3, no. 6, 1973.

[21] U. Kandaswamy, D. A. Adjeroh, and M. C. Lee, "Efficient texture analysis of SAR imagery," *IEEE Transactions on Geoscience and Remote Sensing*, vol. 43, no. 9, pp. 2075–2083, 2005.

[22] S. Beucher, "The Watershed Transformation Applied to Image Segmentation," *Proceedings of the 10th Pfefferkorn Conference on Signal and Image Processing in Microscopy and Microanalysis*, pp. 299–314, 1992.

[23] P. Neubert and P. Protzel, "Compact watershed and preemptive SLIC: On improving trade-offs of superpixel segmentation algorithms," *Proceedings - International Conference on Pattern Recognition*, pp. 996–1001, 2014.

[24] R. Achanta, A. Shaji, K. Smith, A. Lucchi, P. Fua, and S. Susstrunk, "Slic superpixels compared to state-of-the-art superpixel methods," *IEEE Trans. Pattern Anal. Mach. Intell.*, vol. 34, pp. 2274–2282, Nov. 2012.

[25] P. F. Felzenszwalb and D. P. Huttenlocher, "Efficient Graph-Based Image Segmentation," *International Journal of Computer Vision*, vol. 59, no. 2, pp. 167–181, 2004.